

Improved Intensity Inhomogeneity Correction Techniques in MR Brain Image Segmentation

László Szilágyi*, László Dávid*, Sándor M. Szilágyi*,
Balázs Benyó**, Zoltán Benyó**

*Faculty of Technical and Human Sciences, Sapientia – Hungarian Science University of Târgu-Mureş,
Romania (Tel: +40-747-352560; e-mail: {lalo,ldavid,szs}@sapientia.ro).

**Department of Control Engineering and Information Technology, Budapest University of
Technology and Economics, Budapest, Hungary (e-mail: benyo@mit.bme.hu, benyo@jit.bme.hu)

Abstract: Intensity inhomogeneity or intensity non-uniformity (INU) is an undesired phenomenon that represents the main obstacle for MR image segmentation and registration methods. Various techniques have been proposed to eliminate or compensate the INU, most of which are embedded into clustering algorithms. This paper proposes a pre-filtering technique for Gaussian and impulse noise elimination, and a smoothening filter that assists the fuzzy c-means (FCM) algorithm at the estimation of inhomogeneity as a slowly varying additive or multiplicative noise. The segmentation is produced by FCM algorithm together with the INU estimation. The slowly varying behaviour of the bias or gain field is assured by a smoothening filter that performs a context dependent averaging, based on a morphological criterion. The experiments using 2-D synthetic phantoms and real MR images show, that the proposed method provides accurate segmentation. The produced segmentation and fuzzy membership values can serve as excellent support for 3-D registration and segmentation techniques.

1. INTRODUCTION

Magnetic resonance imaging (MRI) is a very popular medical imaging technique, mainly because of its high resolution and contrast, which represent great advantage above other diagnostic imaging modalities. Besides all these good properties, MRI also suffers from three considerable obstacles: noises (mixture of Gaussian and impulse noises), partial volume artefacts (pixels containing at least two types of tissues), and intensity inhomogeneity (Siyal and Yu, 2005). This latter one, also known as intensity non-uniformity (or INU artefact), manifests as a spatially slowly varying function, that makes pixels belonging to the same tissue be observed having different intensities. In order to produce a correct segmentation or registration of MR images, the INU artefact needs to be modelled and compensated.

INU has two different types of sources: those related to the MRI device, and those related to the imaged patient's shape, position and orientation. While the first type of source has efficient compensation and calibration methods, the second type of INU artefacts are much more difficult to handle (Vovk et al., 2007). A widely used technique, handling mostly the first type of INU, consists of the usage of a uniform phantom to produce prior information (Axel et al., 1987).

Homomorphic filtering represents a popular compensation method (Johnston et al., 1996; Brinkmann et al., 1998), built on the theoretical assumption, that the frequency spectra of the image structures and of the INU artefact are non-overlapping each other. The efficiency of such methods are limited because the initial assumption does not hold.

Although several INU compensation approaches exist (Leemput et al., 1999; Pham and Prince, 1999b; Zhang et al., 2001), one of the most widely used methods is the adaptation of the fuzzy c-means (FCM) clustering algorithm to iteratively approximate the INU as a smooth varying bias or gain field. In this order, Pham and Prince (1999a, 1999b) introduced a modified objective function producing bias field estimation and containing extra terms that force this artefact vary smoothly. They also provided a multigrid technique to speed up the computationally heavy algorithm, but even this way, the algorithm performs slowly. A probabilistic approach leading to the same objective function was given in (Li et al., 2005). Liew and Hong (2003) created a log bias field estimation technique that models the INU with smoothing B-spline surfaces.

Further FCM-based bias field estimation techniques were introduced recently by Ahmed et al. (2002) and Siyal and Yu (2005). The modification introduced by Ahmed et al. allows the labelling of a voxel to be influenced by its immediate neighbours. This approach has reduced some of the complexity of its ancestors, but the zero gradient condition that was used for bias field estimation leads to several misclassifications (Siyal and Yu, 2005). The other approach provided a mean spread filtering method to smoothen the estimated bias field in every cycle of the FCM algorithm. This approach reduces the amount of necessary computations, but the result of the segmentation is not deterministic due to the nature of the smoothening filter.

In this paper we propose two filtering techniques to accompany the FCM-based bias- or gain field estimation of the intensity inhomogeneity, and show their efficiency in MR

brain image segmentation using real MR slices and artificial phantoms.

The rest of the paper is organized as follows: section 2 describes the proposed filtering techniques and the FCM-based bias- and gain field estimation approaches. Section 3 provides a qualitative analysis and short discussion of segmentation results. In section 4 the conclusions are formulated.

2. METHODS

2.1. Context dependent pre-filtering

Impulse and Gaussian noise is removed from the original MR image using a context dependent local filtering, which combines averaging and median filtering effects based on physical distances and grey level differences between neighbour pixels.

The proposed technique acts like a low-pass masking, but the mask weights are separately computed for each pixel, based on the distances and grey level differences encountered within a neighbourhood. The weight of each neighbouring pixel is the product of two terms: a distance term that decreases exponentially with Euclidean distance measured from the middle pixel; and a grey level term, which is high for pixels that have similar intensities with the middle pixel and low if they differ significantly. The middle pixel gets its weight based on the reliability of its grey level intensity. Details of such techniques are described in (Cai *et al.*, 2007; Szilágyi *et al.*, 2007).

2.2. Conventional FCM clustering and derivations

The conventional FCM algorithm has been applied successfully in a wide variety of clustering problems. This algorithm optimally partitions a set of object data into a previously set number of c clusters based on the iterative minimization of a quadratic objective function. When applied to segment greyscale images, FCM clusters the intensity value of each pixel x_k , $k=1..n$. The objective function to be minimized is given as follows:

$$J_{FCM} = \sum_{i=1}^c \sum_{k=1}^n u_{ik}^m \|x_k - v_i\|^2, \quad (1)$$

where $m > 1$ is the fuzzy exponent or fuzzyfication parameter, v_i represents the centroid or prototype of the i th cluster, and $u_{ik} \in [0,1]$ is the fuzzy membership function indicating the degree to which pixel k belongs to cluster i . The definition of fuzzy logic implies, that $\sum_{i=1}^c u_{ik} = 1$. The constrained optimization of the objective function is achieved using Lagrange multipliers. In this order, we need to minimize the following function:

$$F_{FCM} = \sum_{i=1}^c \sum_{k=1}^n u_{ik}^m \|x_k - v_i\|^2 - \sum_{k=1}^n \lambda_k \left(1 - \sum_{i=1}^c u_{ik} \right), \quad (2)$$

which we obtained by adding a zero term to the objective function. The minimization is reached by alternately applying the optimization of F_{FCM} over $\{u_{ik}\}$ with v_i fixed, $i=1..c$, and the optimization of F_{FCM} over $\{v_i\}$ with u_{ik} fixed, $i=1..c$, $k=1..n$ (Bezdek and Pal, 1991). In each cycle, optimal fuzzy membership and optimal centroid values are computed using the formulas:

$$u_{ik}^* = \frac{\|x_k - v_i\|^{-2/(m-1)}}{\sum_{j=1}^c \|x_k - v_j\|^{-2/(m-1)}} \quad (3)$$

and

$$v_i^* = \frac{\sum_{k=1}^n u_{ik}^m x_k}{\sum_{k=1}^n u_{ik}^m}. \quad (4)$$

for any $i=1..c$ and $k=1..n$. After adequate initialization of cluster prototype values v_i , (3) and (4) are alternately applied until the norm of the variation of the vector \mathbf{v} , composed of the centroid values, stays within a previously set bound ε .

The above presented algorithm clusters the set of data $\{x_k\}$, which was recorded among ideal circumstances, containing no noise. However, in the real case, the observed data $\{y_k\}$ differs from the actual one $\{x_k\}$: there are impulse and Gaussian noises, which were treated in the previous subsection, and there is the intensity non-uniformity (INU) artefact, which will be handled here.

Literature recommends two different data variation models for intensity inhomogeneity: the bias and the gain field model. If we consider the INU as a bias field, for each pixel k we will have $y_k = x_k + b_k$, where b_k represents the bias value at pixel k . In case of gain field modelling, there will be a gain value g_k for each pixel k , such that $y_k = g_k x_k$. In case of both models, the variation of the intensity between neighbour pixels has to be slow. This is assured by the smoothing filter presented in the next section.

In case of modelling INU as a bias field, the objective function becomes:

$$J_b = \sum_{i=1}^c \sum_{k=1}^n u_{ik}^m \|y_k - b_k - v_i\|^2. \quad (5)$$

Taking the derivatives of the Lagrange multiplier formula that corresponds to J_b , with respect to u_{ik} , v_i and b_k , respectively, and equalling them to zero, we obtain the following optimization formulas:

$$u_{ik}^* = \frac{\|y_k - b_k - v_i\|^{-2/(m-1)}}{\sum_{j=1}^c \|y_k - b_k - v_j\|^{-2/(m-1)}}, \quad (6)$$

$$v_i^* = \frac{\sum_{k=1}^n u_{ik}^m (y_k - b_k)}{\sum_{k=1}^n u_{ik}^m}, \quad (7)$$

$$b_k^* = y_k - \frac{\sum_{i=1}^c u_{ik}^m v_i}{\sum_{i=1}^c u_{ik}^m}. \quad (8)$$

If we approximate the INU artefact as a gain field, the objective function should be:

$$\bar{J}_g = \sum_{i=1}^c \sum_{k=1}^n u_{ik}^m \|y_k / g_k - v_i\|^2. \quad (9)$$

Because the derivatives of this function are hard to handle, we slightly modify this objective function the following way:

$$J_g = \sum_{i=1}^c \sum_{k=1}^n u_{ik}^m \|y_k - g_k v_i\|^2. \quad (10)$$

This approach distorts the function such a way, that it gives higher impact to lighter pixels (as their gain field value will probably be over unity). Taking the derivatives of the Lagrange multiplier that corresponds to J_g , with respect to u_{ik} , v_i and g_k , respectively, and equalling them to zero, we obtain the following optimization formulas:

$$u_{ik}^* = \frac{\|y_k - g_k v_i\|^{-2/(m-1)}}{\sum_{j=1}^c \|y_k - g_k v_j\|^{-2/(m-1)}}, \quad (11)$$

$$v_i^* = \frac{\sum_{k=1}^n u_{ik}^m g_k y_k}{\sum_{k=1}^n u_{ik}^m g_k^2}, \quad (12)$$

$$g_k^* = y_k \frac{\sum_{i=1}^c u_{ik}^m v_i}{\sum_{i=1}^c u_{ik}^m v_i^2}. \quad (13)$$

Similarly to the conventional FCM, these optimization formulas are applied alternatively in each iteration.

2.3. Smoothing filter

The intensity inhomogeneity artefact varies slowly along the image. This property is ignored by both the bias or gain field approaches presented above. To avoid this problem, a filtering technique is applied in each computation cycle, to smoothen the bias or gain field. This filtering introduces an extra step into each optimization cycle, after proceeding with (8) or (13).

Several, not only FCM-based INU compensation approaches apply large sized, 11-31 pixels wide averaging filters performed once or several times in each cycle (Wells *et al.*, 1996; Zhao *et al.*, 2007). These filters efficiently hide tissue details, which may appear in the estimated b_k or g_k values, but also transfer bias or gain components to distantly situated pixels. Using larger averaging windows amplifies this latter undesired effect. In order to reduce the transfer of bias data to distant pixels, we need to check the necessity of averaging at all locations, and decide to proceed or skip the averaging accordingly. Averaging is declared necessary or not, based on the maximum intensity difference encountered within a small neighbourhood of the pixel. The computation of the maximum difference is accomplished by a morphological

gradient operation using a 3×3 square or slightly larger cross-shaped structuring element. Wherever the morphological gradient value exceeds the previously set threshold value θ , the averaged bias or gain value will be used; otherwise the estimated value is validated. The proposed filter can be easily implemented and efficiently performed by batch-type image processing operations.

2.4. Multi-stage bias and gain field estimation

Bias or gain field estimation using the previous FCM-based approaches (Ahmed *et al.*, 2002; Siyal and Yu, 2005; Zhao *et al.*, 2007) can only handle the INU artefact to a limited amplitude. For any pixel, the FCM algorithm assigns the highest fuzzy membership to the closest cluster. Consequently, when the INU amplitude is comparable with the distance between clusters, these pixels will be attracted by the wrong cluster, and the bias or gain field will be estimated accordingly. The smoothening of the bias and gain field may repair this kind of misclassifications, but the larger these wrongly labelled spots are, the harder will be to eliminate them via smoothening.

In order to deal with high-amplitude INU artefacts, we propose performing the bias or gain field estimation in multiple stages. When the FCM-based algorithm given by (6)-(8) of (11)-(13) has converged, we modify the input (observed) image according to the estimated bias or gain field:

$$y_k = y_k^{(old)} - b_k, \text{ or } y_k = y_k^{(old)} / g_k, \quad (14)$$

and then restart the algorithm from the beginning, using the modified input image.

2.5. Algorithm

The presented algorithm can be summarized as follows:

1. Remove the Gaussian and impulse noises from the MR image using the context dependent pre-filtering technique.
2. Initialize cluster prototypes v_i with random values that differ from each other.
3. Initialize the bias (gain) field values with 0-mean (1-mean) random numbers having reduced variance, or simply set $b_k = 0$ ($g_k = 1$) for any pixel k .
4. Compute new fuzzy membership function values u_{ik} , $i = 1 \dots c$, $k = 1 \dots n$, using (6) or (11),.
5. Compute new cluster prototype values v_i , $i = 1 \dots c$, using (7) or (12).
6. Perform new bias or gain field estimation for each pixel k using (8) or (13).
7. Smoothen the bias or gain field using the proposed smoothening filter.

8. Repeat steps 4-7 until there is no relevant change in the cluster prototypes. This is tested by comparing any norm of the difference between the new and the old vector \mathbf{v} with a preset small constant ϵ .

9. Modify the input image according to the estimated bias or gain field using (14), and repeat steps 2-8 until the INU artefact is compensated. The algorithm usually requires a single repetition.

3. RESULTS AND DISCUSSION

We applied the presented filtering and segmentation techniques to several T1-weighted real MR images, artificially contaminated with different kinds of noises. Fig. 1. demonstrates the efficiency of the pre-filtering technique on a real MR slice taken from Internet Brain Segmentation Repository (Worth, 2000).

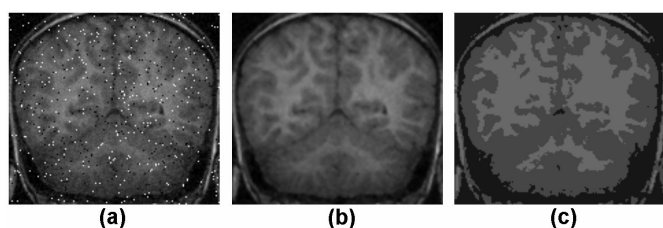


Fig. 1. Elimination of impulse and Gaussian noises demonstrated with a real T1-weighted MR brain image contaminated with artificial noise: (a) original, (b) filtered, (c) FCM segmentation after correction

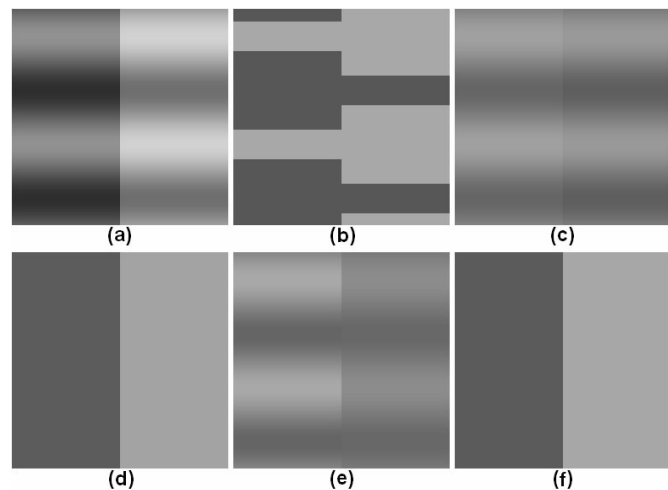


Fig. 2. Inhomogeneity correction using a phantom: (a) original, (b) FCM segmentation result without correction, (c) estimated bias field, (d) segmentation result based on bias field estimation, (e) estimated gain field, (d) segmentation result based on gain field estimation

The results of bias and gain field estimation performed on a phantom image are shown in Fig. 2. Conventional FCM is unable to compensate the INU artefact, but with the use of smoothed bias or gain field, this phenomenon is efficiently overcome.

In case of low-amplitude inhomogeneity, a single stage of bias or gain field estimation is sufficient. Fig. 3. shows the

accuracy and efficiency of the proposed segmentation technique, using a real T1-weighted MR brain slice. The presence of the smoothing filter supports the accurate segmentation, while the pre-filter has a regularizer effect on the final result.

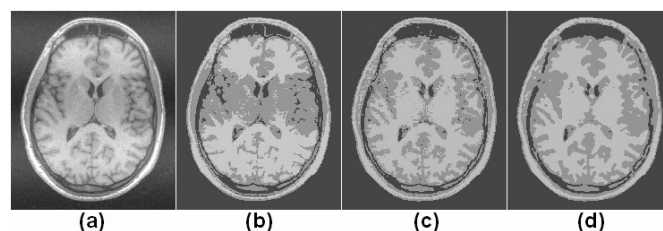


Fig. 3. Inhomogeneity correction demonstrated on an artificially contaminated real MR image: (a) original, (b) FCM segmentation without correction, (c) result of FCM-based segmentation with no pre-filtering, (d) result of FCM-based segmentation with context sensitive pre-filtering

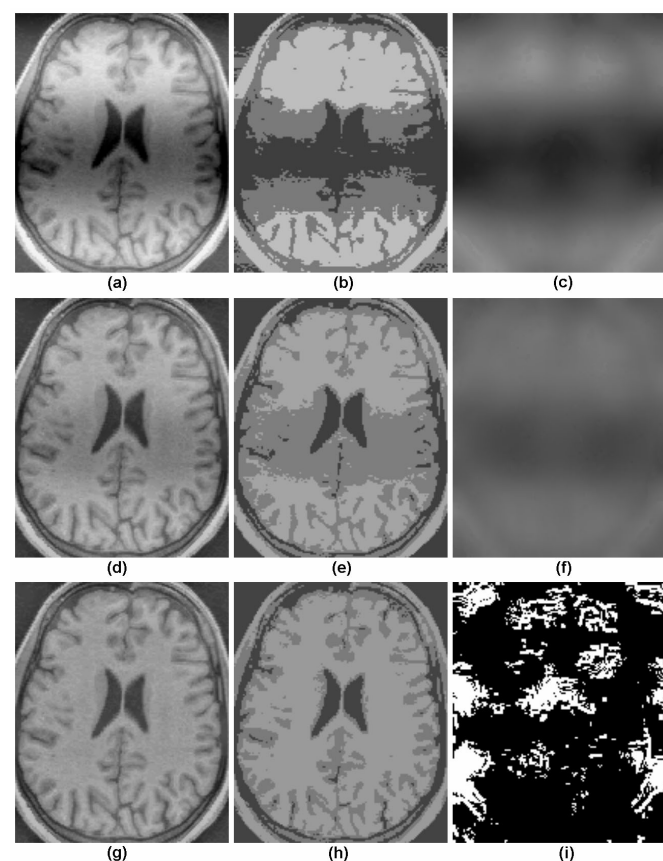


Fig. 4. Segmentation of a heavily inhomogeneous real MR image: (a) original, (b) segmentation without compensation, (c) bias field estimated in the first stage, (d) compensated MR image after first stage, (e) FCM-based segmentation after first stage, still unusable, (f) bias field estimated in the second stage, (g) final compensated image, (h) segmented image, (i) a smoothing mask computed by the proposed filter

Fig. 4. shows the intermediary and final result of a segmentation process, performed on a heavily INU-contaminated MR image. The inhomogeneity correction succeeds after two stages. Fig. 4(i) shows the behaviour of the proposed filtering technique: white pixels indicate places

which required averaging in a given computational cycle, while black ones signifies those places where averaging was unnecessary.

Table 1. Misclassification rates (in %) with various smoothing filters, in case of heavily INU-contaminated MR images

Structuring element	Averaging window size 11		Averaging window size 19	
	once	3 times	Once	3 times
Averaging	7.357	5.766	4.368	7.141
3×3 square	6.281	6.201	2.852	3.379
5×5 cross	6.711	5.674	3.873	3.938
7×7 cross	6.254	5.518	3.470	5.029
11×11 cross	6.351	4.432	3.271	6.437

Table 1. shows the misclassification percentages of the proposed INU compensation and MR image segmentation method, depending on the size of the averaging window expressed in pixels, the structuring element of the morphological criterion of the proposed filter, and the number of smoothing iterations performed in each cycle of the modified FCM algorithm. The experimental data reveal that the proposed filtering technique improves the segmentation quality assured by the averaging filter. The best segmentation was obtained using a 3×3 square shaped structuring element used by the morphological criterion, combined with averaging using a window size of 19×19 pixels.

Using several repetitive stages during INU compensation may reduce the intensity difference between tissue classes, which leads to misclassifications. That is why the estimation is limited to two steps, performing several stages is not recommendable.

4. CONCLUSIONS

A novel smoothing filter has been proposed to assist bias or gain field estimation embedded into the conventional FCM algorithm scheme. The proposed method proved to segment accurately and efficiently MR images in the presence of intensity non-uniformity. Although the proposed method segments 2-D MR brain slices, it gives a relevant contribution to the accurate volumetric segmentation of the brain, because the segmented images and the obtained fuzzy memberships can serve as excellent input data to any level set method that constructs 3-D cortical surfaces. Further works aim at developing a context sensitive pre-filter for the elimination of INU artefacts, too, so that the segmentation can be performed using a histogram-based quick FCM algorithm.

ACKNOWLEDGEMENTS

This research was supported in part by the Hungarian National Research Funds (OTKA) under Grant No. T069055, the Hungarian National Office for Research and Technology

(NKTH), the Sapientia Institute for Research Programs (KPI), and the Communitas Foundation.

REFERENCES

- Ahmed, M.N., S.M. Yamany, N. Mohamed and A.A. Farag (2002). A modified fuzzy c-means algorithm for bias field estimation and segmentation of MRI data. *IEEE Trans. Med. Imag.*, **21**, 193–199
- Axel, L., J. Costanini, and J. Listerud (1987). Inhomogeneity correction in surface-coil MR imaging. *Amer. J. Roentgenol.*, **148**, 418–420
- Bezdek, J.C. and S.K. Pal (1991). *Fuzzy models for pattern recognition*. IEEE Press, Piscataway, NJ.
- Brinkmann, B.H., A. Manduca and R.A. Robb (1998). Optimized homomorphic unsharp masking for MR grayscale inhomogeneity correction. *IEEE Trans. Med. Imag.*, **17**, 161–171
- Cai, W., S. Chen, and D.Q. Zhang (2007). Fast and robust fuzzy c-means algorithms incorporating local information for image segmentation. *Patt. Recogn.* **40**, 825–838
- Johnston, B., M.S. Atkins, B. Mackiewicz, and M. Anderson (1996). Segmentation of multiple sclerosis lesions in intensity corrected multispectral MRI. *IEEE Trans. Med. Imag.*, **15**, 154–169
- Leemput, K.V., F. Maes, D. Vandermeulen and P. Suetens (1999). Automated model-based bias field correction of MR images of the brain. *IEEE Trans. Med. Imag.*, **18**, 885–896
- Li, X., L.H. Li, H.B. Lu and Z.G. Liang (2005). Partial volume segmentation of brain magnetic resonance images based on maximum a posteriori probability. *Med. Phys.*, **32**, 2337–2345
- Liew, A.W.C. and Y. Hong (2003). An adaptive spatial fuzzy clustering algorithm for 3-D MR image segmentation. *IEEE Trans. Med. Imag.*, **22**, 1063–1075
- Pham, D.L. and J.L. Prince (1999a). Adaptive fuzzy segmentation of magnetic resonance images. *IEEE Trans. Med. Imag.*, **18**, 737–752
- Pham, D.L. and J.L. Prince (1999b). An adaptive fuzzy C-means algorithm for image segmentation in the presence of intensity inhomogeneity. *Patt. Recogn. Lett.*, **20**, 57–68
- Siyal, M.Y. and L. Yu (2005). An intelligent modified fuzzy C-means based algorithm for bias field estimation and segmentation of brain MRI. *Patt. Recogn. Lett.*, **26**, 2052–2062
- Szilágyi, L. (2006). Medical Image Processing Methods for the Development of a Virtual Endoscope. *Periodica Polytechnica Ser. El. Eng.*, **50**, 69–78
- Szilágyi, L., S.M. Szilágyi and Z. Benyó (2007). Efficient Feature Extraction for Fast Segmentation of MR Brain Images. *Lect. Notes Comp. Sci.*, **4522**, 611–620

- Vovk, U., F. Pernuš, and B. Likar (2007). A review of methods for correction of intensity inhomogeneity in MRI. *IEEE Trans. Med. Imag.*, **26**, 405–421
- Wells, W. M., W. E. L. Grimson, R. Kikinis, and F. A. Jolesz (1996). Adaptive segmentation of MRI data. *IEEE Trans. Med. Imag.*, **15**, 429–442
- Worth, A. (2000) Internet Brain Segmentation Repository. <http://www.cma.mgh.harvard.edu/ibsr>.
- Zhang, Y., M. Brady, and S. Smith (2001). Segmentation of brain MR images through a hidden Markov random field model and the expectation-maximization algorithm. *IEEE Trans. Med. Imag.*, **20**, 45–57
- Zhao, Q., J. Song, and Y. Wu (2007). Improved fuzzy c-means segmentation algorithm for images with intensity inhomogeneity. *Adv. Soft Computing*, **41**, 150–159